Design Exploration of a Slotted-Wing Common Research Model

Brett R. Hiller[1], Richard L. Campbell[2], and Michelle N. Lynde[3]
NASA Langley Research Center, Hampton, VA, 23681

A knowledge-based aerodynamic design method, Constrained Direct Iterative Surface Curvature (CDISC), has been leveraged for the computational design exploration of a Common Research Model with Reduced-Sweep and Slotted Wings (CRMRS-SW). Cruise-slotted-wing airfoils include a slot near the trailing edge of a main airfoil component to introduce stream air to the low-momentum, upper-surface boundary layer on a flap airfoil component with the goal of allowing for a more aft loading, relative to supercritical airfoils, without shock-induced separation. Ultimately, the cruise slotted wing is a passive technology that allows for an increase in the drag divergence Mach number and/or an increase in aerodynamic efficiency at a given cruise condition. These aerodynamic benefits may be realized at the vehicle level through a tradespace that includes the following design options: increasing cruise Mach number, increasing wing thickness, decreasing wing sweep, increasing lift coefficient and/or decreasing drag coefficient. The present study aimed to evaluate the slotted-wing concept's potential as a drag-saving technology in application to a single-aisle transonic transport aircraft at a given cruise condition. The CDISC design method was used to develop a better understanding of the slotted-wing design variables that have a significant impact on the variability in aircraft drag and leverage this newly-developed knowledge to quantify the aerodynamic performance benefits enabled by the cruise slotted wing.

Nomenclature

c	=	Chord, inches
C_D	=	Drag coefficient
C_L	=	Lift coefficient
c_l	=	Sectional lift coefficient
c_m	=	Sectional pitching moment coefficient
C_p	=	Pressure coefficient
D	=	Drag, pounds-force
L	=	Lift, pounds-force
M	=	Mach number
$(r/c)_{LE}$	=	Leading-edge radius normalized by local chord
Re_{MAC}	=	Reynolds number based on mean aerodynamic chord
$(t/c)_{max}$	=	Maximum thickness-to-chord ratio
V_1	=	Midchord pressure gradient parameter in target pressure architecture
x/c	=	x-location nondimensionalized by local chord
X_{acc}	=	x/c location of end of rapid leading-edge acceleration in target pressure architecture
X_{shk}	=	x/c location of shock location in target pressure architecture
z/c	=	z-location nondimensionalized by local chord
α	=	Angle of attack, degrees
η	=	y-location nondimensionalized by semispan
ϕ	=	Twist, degrees

[1]Research Aerospace Engineer, NASA Langley Research Center, Mail Stop 499, Hampton, VA 23681, AIAA Member.
[2]Senior Research Engineer, NASA Langley Research Center, Mail Stop 499, Hampton, VA 23681, AIAA Associate Fellow.
[3]Research Aerospace Engineer, NASA Langley Research Center, Mail Stop 499, Hampton, VA 23681, AIAA Member.

I. Introduction

Given the desire to reduce the environmental impact of commercial transport aircraft, the aerospace industry is in continuous pursuit of configurations and technologies aimed at significantly reducing the noise, emissions, and fuel consumption of next-generation vehicles. In particular, fuel consumption reductions may be achieved by reducing an aircraft's empty weight and/or increasing its aerodynamic cruise efficiency, ML/D [1]. One potential concept targetting efficiency improvements is the cruise slotted wing. A cruise-slotted-wing airfoil consists of two components: a main component in the forward-chord region and a flap component in the aft-chord region. Illustrated in Fig. 1, slotted airfoils include a slot between the upper and lower surfaces near the trailing edge of the main airfoil component to introduce stream air to the low-momentum, upper-surface boundary layer on the flap airfoil component with the goal of allowing for a more aft loading, relative to supercritical airfoils, without shock-induced separation. These aerodynamic flowfield benefits may be realized at the vehicle level through a tradespace that includes the following design options: increasing cruise Mach number, increasing wing thickness, decreasing wing sweep, increasing lift coefficient and/or decreasing drag coefficient. In the first design scenario, increasing the drag rise Mach number would allow for an aircraft to cruise at a higher speed with a limited increase in total aircraft drag. Alternatively, the slotted wing could permit a thicker wing, which would allow for a lighter wing structure and greater fuel volume. The reduced-sweep design scenario would offer both a lighter wing structure and a greater potential for natural laminar flow due to the inherent ability to suppress the growth of modal instabilities that often lead to turbulent transition [2]. Increasing the lift coefficient would enable increased weight, such as fuel for longer duration missions, or cruise at a higher altitude. Finally, decreasing the drag coefficient would inherently lead to reduced fuel consumption and an increased range.

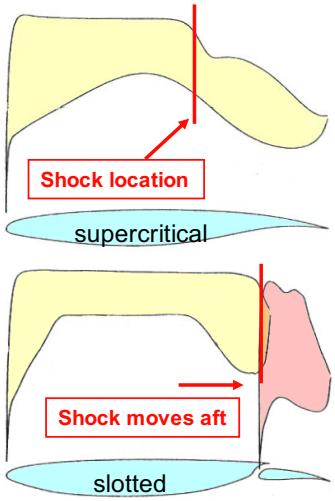

Figure 1. Notional pressure distributions for supercritical and slotted airfoils at cruise[3].

The cruise slotted wing was originally proposed in 1965 by Richard Whitcomb and Larry Clark of the National Aeronautics and Space Administration (NASA) Langley Research Center as a technology that could be paired with the well-known supercritical airfoil to increase the drag rise Mach number and allow for higher cruise speeds for commercial aircraft [4]. Whitcomb and Clark primarily relied on intuitive reasoning to design a slotted, supercritical airfoil based on the five following objectives: (1) maximize the Mach number at which the shock moves aft of the slot exit, (2) minimize boundary-layer separation on the upper and lower airfoil surfaces up to the drag rise Mach number, (3) minimize shock losses above the upper surface at the cruise Mach number, (4) minimize skin-friction drag due to the slot, and (5) provide satisfactory off-design performance. Wind tunnel tests conducted in the Langley 8-Foot Transonic Pressure Tunnel were able to substantiate the expected aerodynamic performance of the slotted airfoil with an increase in the drag rise Mach number from 0.67 to 0.79 at the design section lift coefficient with only a 10% increase in drag relative to a traditional National Advisory Committee for Aeronautics (NACA) 642A215 airfoil. Remarkably, these improvements in aerodynamic efficiency were attained without the use of computational design methods to optimally shape the main and flap airfoil components. Continued research found that boundary-layer separation up to the design Mach number could be drastically reduced without the use of a slot by tailoring the upper surface pressure distribution alone [5]. Due to its relative simplicity, the integral supercritical airfoil has become routinely used in commercial transports since the 1970s as a means of increasing cruise Mach number [6].

Compared to the supercritical airfoil, a slotted airfoil would theoretically permit a greater loading in the aft region of the airfoil by recovering the pressure gradient over the wake as opposed to the upper surface boundary layer, which would permit reduced loading on the main element and pursuit of the previously mentioned design trades. With the maturation of Computational Fluid Dynamics (CFD) and the development of computational design methods, several efforts have been made since the 1990s to further assess the potential benefits of the slotted airfoil. In 1993, Mark Drela of the Massachusetts Institute of Technology used MSES, an Euler/Boundary-layer flow solver, to perform a multipoint design optimization of a two-element slotted airfoil [7]. The baseline slotted airfoil was first designed by a computational cut-and-try approach, resulting in a considerably higher lift coefficient relative to single-element airfoils at the cruise Mach number. The subsequent optimization process achieved further drag reductions across a 16-point Mach number sweep for improved off-design performance. This effort highlighted the benefits of leveraging computational methods for slotted airfoil design exploration, as well as the technology's continued potential for performance improvements.

In the early 2000s, collaborative research between Boeing and NASA Langley was conducted to verify the performance benefit for full-span [8] and partial-span [9] slotted wing commercial transports via CFD analyses and wind tunnel tests. A partial-span slotted wing was successfully designed, producing a cruise speed increment of $\Delta M = 0.025$ with a 1% improvement in aerodynamic efficiency relative to a conventional transonic wing. While the design provided satisfactory high-lift and stability and control characteristics, it was noted that reducing the skin-friction drag penalty during climb would be desirable. Noted technical challenges included the slot sensitivity to small changes, structural complexity due to slot brackets, and accurate load predictions on the flap in the prescence of complex, viscous flow interactions [3]. The primary recommendation was the need to perform multidisciplinary design to reduce risks for production applications. Furthermore, the study was limited to evaluating the technology's ability to increase the cruise Mach number of a long-range, twin-aisle aircraft without considering alternative performance-measure benefits or its applicability to slower cruising configurations.

More recently, a series of Slotted Natural-Laminar-Flow (SNFL) airfoils have been designed and analyzed theoretically by Dan Somers of Airfoils Incorporated for rotorcraft [10], general aviation [11], business jets [12], and transport aircraft [13] applications. In contrast to previous designs, these airfoils target profile drag reductions by tailoring pressure distributions to allow for natural laminar flow on both the upper and lower surfaces of the main element. As part of a NASA University Leadership Initiative (ULI), computational analyses and low-speed wind tunnel tests have been completed to further investigate the performance of the rotorcraft [14, 15] and light business jet [16] airfoils. Results have demonstrated an ability of the airfoils to achieve a higher maximum lift coefficient and lower profile-drag coefficient, but at the expense of unsatisfactory stall characteristics. Nonetheless, the slotted airfoil remains an intriguing technology due to its demonstrated potential for aerodynamic efficiency improvements. Moving forward, computational design studies capable of resolving the complex, three-dimensional viscous flow interactions for high-speed configurations would help to better quantify the aerodynamic performance of slotted wings, to improve our understanding of optimal airfoil shape parameters, and to investigate the multiobjective design tradespace.

The overarching goal of this research is to improve confidence in the application of the cruise slotted wing concept to single-aisle commercial transport configurations. Toward this effort, a new generic baseline configuration was created by reducing the sweep of the Common Research Model (CRM) [17] for a corresponding cruise Mach number of $M = 0.8$. The present study aimed to explore and compare the aerodynamic design of conventional- and partial-span slotted-wing (SW) variants of the Common Research Model with Reduced Sweep (CRMRS), designated as CRMRS and CRMRS-SW, respectively. A knowledge-based aerodynamic design method, CDISC, was used in conjunction with the Unstructured Mesh 3D (USM3D) Navier-Stokes flow solver to explore the slotted wing concept's potential for reducing the drag of a single-aisle transonic transport aircraft at given cruise condition. Standard CDISC best practices for transonic transport configurations were used to design the conventional CRMRS. Without the underlying design knowledge for slotted-wing configurations, a two-dimensional parametric grid study was used to rapidly explore the influence of flap design variables on slotted airfoil pressure distributions and evaluate their resulting impact on aerodynamic performance. From this study, new CDISC design constraints were formulated and tested for the turbulent design of the CRMRS-SW configuration at cruise and off-design conditions.

II. Method

A flow chart of the design and analysis process implemented in this work is illustrated in Fig. 2. The process utilizes a flow solver, grid manipulation tools, a design module, transition prediction software, and a drag decomposition program. The primary design and analysis modules are shown in red, whereas auxiliary output information is shown in blue. The design loop (shown on the left) begins with a flow solution for the baseline configuration at the design cruise

condition. Using the baseline CFD grid and flow solution, the extraction module obtains the surface geometry, pressure distribution, and skin-friction data at several spanwise, user-specified design stations along the wing. The design module then modifies the baseline geometry in an attempt to match target pressure distributions defined at each design station.

Once a satisfactory design is generated, a single design performance evaluation (shown on the right) is executed. The transition prediction software is not a requirement for the fully turbulent design considered in this study, but will be used to evaluate the extent of laminar flow permitted by the conventional and slotted-wing designs for the reduced-sweep CRMRS configuration. If warranted, a forced-laminarization USM3D solution may be generated to better quantify the aerodynamic performance of a candidate design. A drag decomposition program then uses the design flow solution to estimate the relative changes in profile drag, wave drag, and skin-friction drag. Overall, the method provides the capability required to explore the impact of various slotted airfoil shape parameters on the variability of the aircraft drag and evaluate the technology's potential based on its aerodynamic performance relative to a conventional wing design.

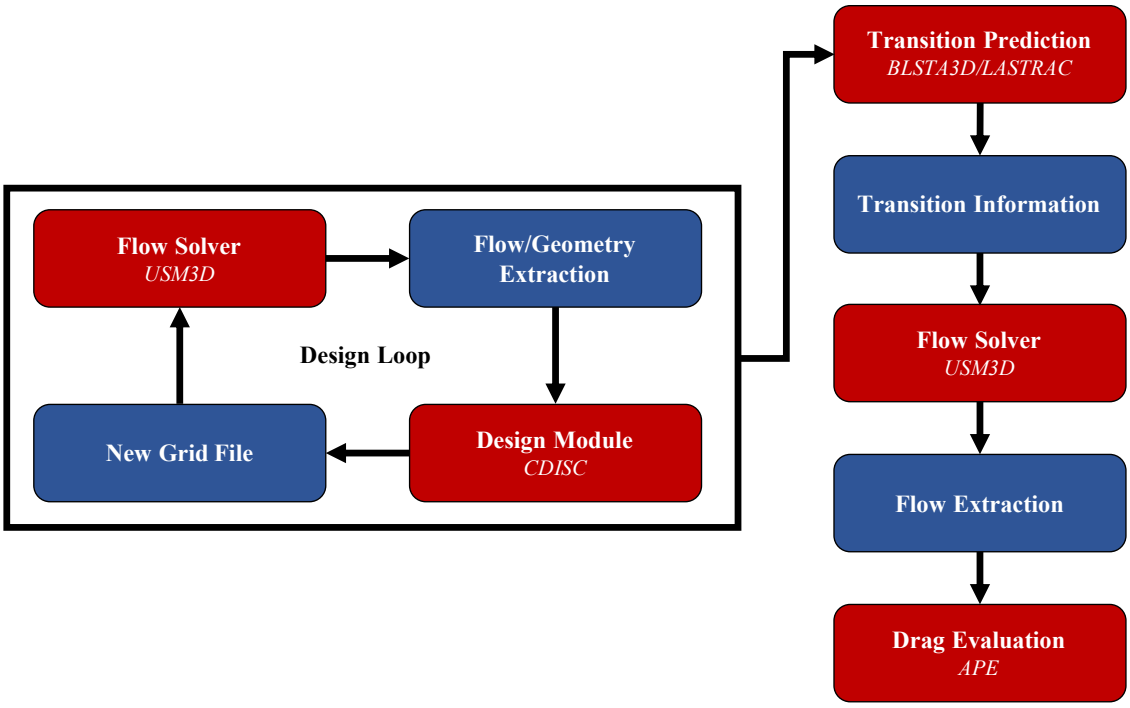

Figure 2. Flow chart of the design and analysis process.

A. Flow Solver

NASA's USM3D, a tetrahedral, cell-centered, Reynolds-averaged Navier-Stokes solver [18], was used to generate steady-state flow solutions. Inviscid fluxes were computed with Roe's flux-differencing scheme. The min-mod flux limiter was used to initialize the transonic, slotted-wing solutions prior to producing a converged solution without flux-limiting. For all of the iterative design solutions, the Spalart-Allmaras one-equation turbulence model was used. For all candidate designs, USM3D's forced-laminarization option may be enforced ahead of any predicted transition fronts to better model the aerodynamic performance. Given that an external boundary layer solver is used to provide the profiles for the laminar flow stability analysis, our standard practice for generating viscous grids could be used.

Tetrahedral computational grids were generated with Pointwise® V18.0 using IGS-formatted, computer-aided-design geometry files for the CRMRS and CRMRS-SW configurations. The aircraft models consist solely of the fuselage and associated wings, where the nacelle, vertical tail, and horizontal stabilizer were removed to enable more rapid analyses. Both configurations share a common inboard wing geometry, while a partial-span slotted-wing is used outboard for the latter. Semispan viscous grids were generated using an initial spacing consistent with a cell-centered y+ of 0.5 based on half of the chord length ($c_{ref}/2$). For both configurations, the leading and trailing edges of the wings were resolved using Pointwise® T-Rex cells, which are layers of anisotropic tetrahedral cells emanating from the boundary curves. To provide comparable grid resolution, the fuselage surface grid and the average node-spacing for the leading and trailing

edges of the wings were identical. For the CRMRS-SW, T-Rex cells were also used on the trailing edge of the main component and leading edge of the flap component. Due to the refinement necessary to resolve the high curvature slot, the CRMRS and CRMRS-SW grids do not have equivalent cell counts but remain in the 50-60 million cell range.

B. Design Module

The design module selected for this study is CDISC [19], a knowledge-based design method compatible with USM3D, among many other 2D/3D flow solvers. CDISC uses flow-geometry sensitivity derivatives, predetermined from empirical and analytical studies, to estimate the geometric changes needed to minimize the difference between current and target pressure distributions. This computationally efficient design approach eliminates the need to numerically calulate sensitivity derivatives and allows the design to converge in parallel with the flow solution. Such a method is appropriate in the case of turbulent wing design, for which notional pressure distributions are often known. CDISC flow constraints are available to enforce a variety of engineering design variables, including: sectional force and moment coefficients, spanwise load distributions, and shock location/strength. In addition, geometry constraints are available to address structural and manufacturing requirements, including: thickness, curvature, volume, and leading-edge radius. The requirement for new flow and geometry constraints is to be evaluated in the turbulent design of slotted wings.

C. Transition Prediction

An automated transition prediction process utilizing the Boundary Layer Code for Stability Analysis 3D (BLSTA3D) boundary layer code [20] and the Langley Stability and Transition Analysis Code (LASTRAC) stability analysis software [21] will be leveraged to perform preliminary evaluations of the laminar flow extent of candidate designs. BLSTA3D provides the required boundary layer temperature and velocity profiles for LASTRAC based on the airfoil section geometries used in the design process and their associated pressure coefficient distributions. In addition, the software also provides estimates for the momentum thickness Reynolds number, Re_θ, useful for attachment line assessments. The conical flow option in BLSTA3D is used to simulate both wing sweep and taper. The LASTRAC software provides a range of stability analysis methods, including linear stability theory (LST) to linear and nonlinear parabolized stability equations. In this study, LST computations including compressibility effects are to be generated. It is assumed for the transonic cruise conditions considered that the dominant stability modes are freestream Tollmien-Schlichting (TS) with wave number (β) set to zero, and stationary crossflow (CF) with frequency set to zero. Using the LST method within LASTRAC in conjunction with the n-factor method allows for transition front predictions.

D. Drag Evaluation

Drag evaluations are completed by an in-house Aerodynamic Performance Estimator (APE) code. Using a converged flowfield solution, APE decomposes the total aircraft drag into constituent values of profile drag, skin-friction drag, and wave drag. In providing this information, the sensitivity of slotted-wing design parameters to the variability of total aircraft drag and its various components may be evaluated.

III. Conventional Wing Design

This section reviews the design and analysis of the conventional wing design for the CRMRS. Prior to designing the slotted-wing configuration, it was important to establish a transonic design with aerodynamic performance representative of what is achievable with conventional wings. The following subsections will outline the design strategy implemented within CDISC, as well as cruise and off-design performance for the baseline and designed CRMRS. The design will be generated using a fully turbulent design approach, while the extent of laminar flow will be assessed outside the design loop to better evaluate the aerodynamic performance.

A. Baseline Model and Design Condition

The original CRM was designed as a generic representation of modern twin-aisle transport aircraft [17] to aid CFD validation and computational design research. Since its development, the model has been used in several CDISC studies for both turbulent and natural laminar flow design [22–24]. Given the motivation to improve confidence in the application of the cruise slotted wing concept to single-aisle aircraft, a representative configuration was proposed through modification of the original CRM geometry and scaling of the CRM cruise conditions, based on a decrease in the cruise Mach number from 0.85 to 0.80. The CRMRS configuration was generated by reducing the CRM's quarter-chord sweep from 35° to 27.4° based on simple sweep theory. Identical values are used for the semispan and mean aerodynamic chord (MAC), among other reference quantities. The lift coefficient and Reynolds number based on

MAC were determined to be 0.564 and 20 million, respectively, calculated using a constant altitude scaling. Figure 3 shows a planform view of the CRMRS with a series of 11 equidistant wing design stations designated by black and red lines. CDISC is used to shape the airfoils at each of these wing design stations to match target pressure distributions while satisfying a series of flow and geometry design constraints in an attempt to reduce total aircraft drag.

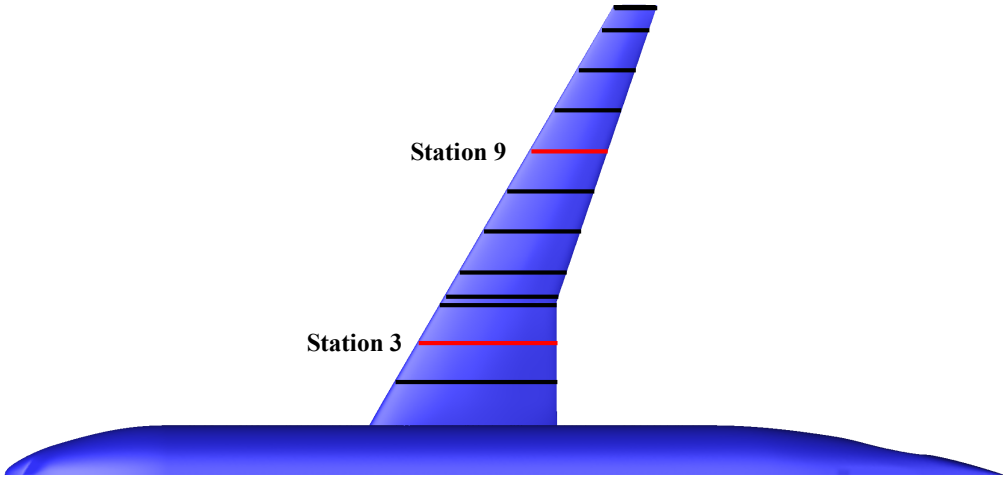

Figure 3. Planform view of the CRMRS with wing design stations designated by black and red lines.

B. Design Strategy

The CDISC design module automatically generates target pressure distributions based on the current analysis pressures and any user-specified flow or geometry constraints. For the CRMRS turbulent design, a single flow constraint was used to create the target pressure distributions at each of the wing design stations. Various parameterizations of this CDISC flow constraint have been previously demonstrated for laminar and turbulent designs at transonic and supersonic flight conditions [23, 24]. A common parameterization of this flow constraint for transonic design is illustrated in Fig. 4. As shown here, the flow on the upper surface is rapidly accelerated to a location X_{acc}, followed by an adverse midchord pressure gradient (V_1) region, ending with a shock located at X_{shk}. This flow constraint was used to design wing stations 2-10, while the root (1) and wingtip (11) design stations were held fixed.

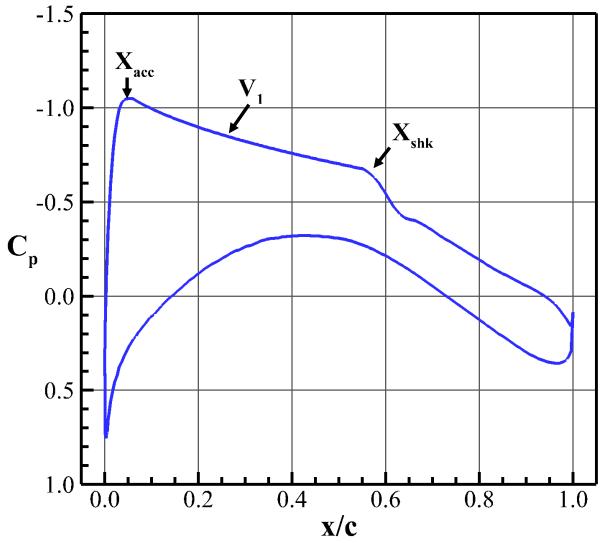

Figure 4. Notional target pressure distribution for CDISC turbulent wing station design.

A summary of the turbulent flow constraint parameter values for each wing design station are listed in Table 1. At every CRMRS wing design station, the value for X_{acc} was set to 0.05c based on empirical design rules for transonic airfoils. By rapidly accelerating the flow near the leading edge, the section lift coefficient can be maintained while permitting a gradual reduction in curvature over the midchord region and a corresponding decrease in the local Mach number ahead of the shock to reduce its strength. The values for V_1 were set based on the results of a previous CRM design study in which CDISC was combined with a simple optimization module to minimize the total aircraft drag by varying the spanwise V_1 values [23]. These gradient values represent a tentative best-practice, where a value of 1.0 is used for the most inboard stations, followed by a relatively linear decrease in V_1 for more outboard wing stations. While these values are unlikely to be optimal for the CRMRS configuration, they should provide a well-designed transonic conventional wing for comparisons to the slotted-wing design. The shock location, X_{shk}/c, was set to a value of 0.60c for the inboard stations (2-4) and a value of 0.65c for the outboard stations (5-10) following the planform break. These are empirically-derived values based on shifting the shock as far aft as possible without causing boundary-layer separation, an effect that is onset more rapidly for the inboard stations due to fuselage interference effects.

Table 1. Turbulent flow constraint parameter values for each wing design station.

Station	2	3	4	5	6	7	8	9	10
$\mathbf{X_{acc}/c}$	0.05	0.05	0.05	0.05	0.05	0.05	0.05	0.05	0.05
$\mathbf{V_1}$	1.00	0.75	0.55	0.50	0.35	0.25	0.20	0.05	-0.01
$\mathbf{X_{shk}/c}$	0.60	0.60	0.60	0.65	0.65	0.65	0.65	0.65	0.65

In terms of constraints for the CRMRS design, the baseline sectional lift coefficient, c_l, and maximum thickness-to-chord ratio, $(t/c)_{max}$, are held constant for each design station. These constraints are enforced in consideration of structural limitations for the baseline aircraft. By holding the lift coefficients constant, reductions in induced drag may be eliminated by preserving the spanwise loading characteristics. By preventing changing in the maximum airfoil thickness, reductions in profile and skin-friction drag may also be eliminated. However, it is important to note that CDISC allows for the location of the maximum airfoil thickness to change while attempting to match target pressure distributions. Overall, CDISC seeks to shape the airfoil to achieve a decrease in total aircraft drag via reductions in wave drag and, potentially, profile drag due to weaker shock strengths.

C. Design Results

Starting from an initial baseline analysis of 10,000 flow solver iterations, 60 design cycles were run with 500 iterations each, for an additional 30,000 iterations or three times the original analysis. Once the design converged to the target pressure distributions, an additional 20 design cycles with 500 iterations each were simulated to only change the configuration angle of attack to match the cruise total lift coefficient. The angle-of-attack values needed to match the lift coefficient were 2.27° and 2.24° for the baseline and design, respectively. Representative results for the inboard and outboard wing regions will be summarized by reviewing the designs at stations 3 and 8, as previously shown in Fig. 3.

Figure 5 shows the pressure distributions and airfoil geometries at design station 3 for the baseline and final design, in addition to the target C_p distribution. Local changes in twist have been removed from the airfoil shapes to more clearly identify the changes in thickness and leading-edge radius. The baseline pressure distribution is characterized by a more than desirable leading-edge acceleration that leads to a more rapid increase in local Mach number. This excessive acceleration leads to a strong shock that terminates abruptly near 0.4c. In contrast, the target distribution reduces the leading-edge acceleration while providing an adverse midchord pressure gradient to allow for a shock at the specified design location of 0.6c. The result is a weaker shock with comparable pressure distributions in the aft-chord region. In reviewing the airfoil shape, it is apparent that the leading-edge radius has decreased to allow for the desired leading-edge acceleration characteristics. Additionally, the location of maximum thickness appears to shift more rearward to provide a reduced midchord curvature, thus, reducing the shock strength and shifting the shock aft.

Figure 6 shows the pressure distributions and airfoil geometries at design station 8 for the baseline and final design, in addition to the target C_p distribution. Again, local changes in twist have been removed to more readily identify airfoil shape changes. Relative to the inboard station, the baseline pressure distribution shows a weaker leading-edge acceleration with less dramatic differences relative to the target acceleration. Additionally, the baseline pressure distribution for the outboard wing is characterized by two shocks at locations of 0.4c and 0.65c. In contrast, the target pressure distribution is characterized by a mild, adverse pressure gradient extending from 0.05c to a single shock located

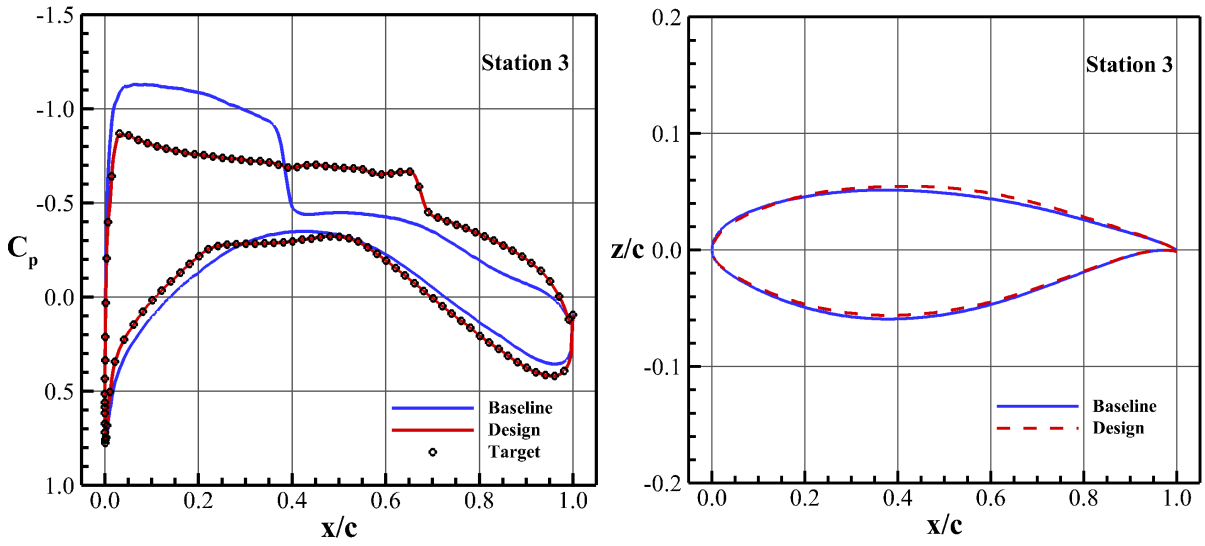

(a) Pressure distributions (b) Airfoil geometries

Figure 5. USM3D results for the CRMRS at Station 3 (η = 0.28). Left shows the baseline, design, and target pressure distributions. Right shows the baseline and design airfoil geometries with local twist removed.

at 0.65c. The resulting decrease in local Mach number leads to a slightly weaker shock relative to the baseline's second shock. The changes in airfoil geometry are less pronounced outboard at design station 8 relative to design station 3, but remain consistent with a slight decrease in leading-edge radius and a shift in maximum thickness rearward.

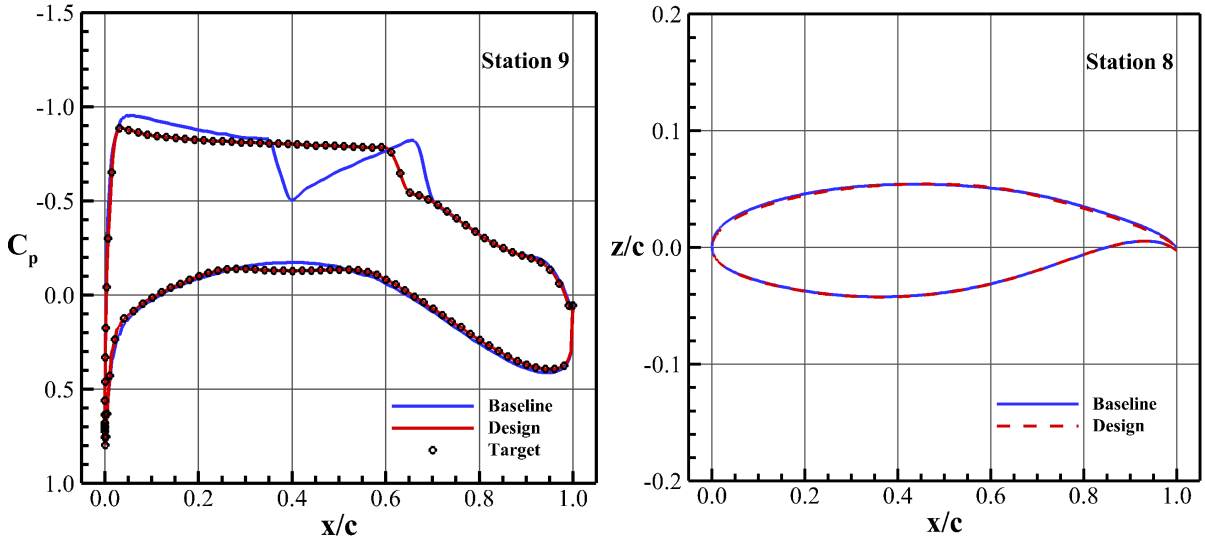

(a) Pressure distributions (b) Airfoil geometries

Figure 6. USM3D results for the CRMRS at Station 8 (η = 0.73). Left shows the baseline, design, and target pressure distributions. Right shows the baseline and design airfoil geometries with local twist removed.

Additional comparisons of the spanwise loading and geometry characteristics between the baseline and design CRMRS configurations are provided in Figs. 7 and 8, respectively. Figure 7 illustrates the sectional lift (c_l) and pitching moment (c_m) coefficients as a function of nondimensional semispan location (η). As mentioned earlier, the sectional lift coefficient of the designed CRMRS was constrained to be identical to the original baseline values. At this time, no sectional pitching moment constraints are enforced, but the values remain relatively close to the baseline values with a slight decrease inboard that is reflective of a small additional aft loading.

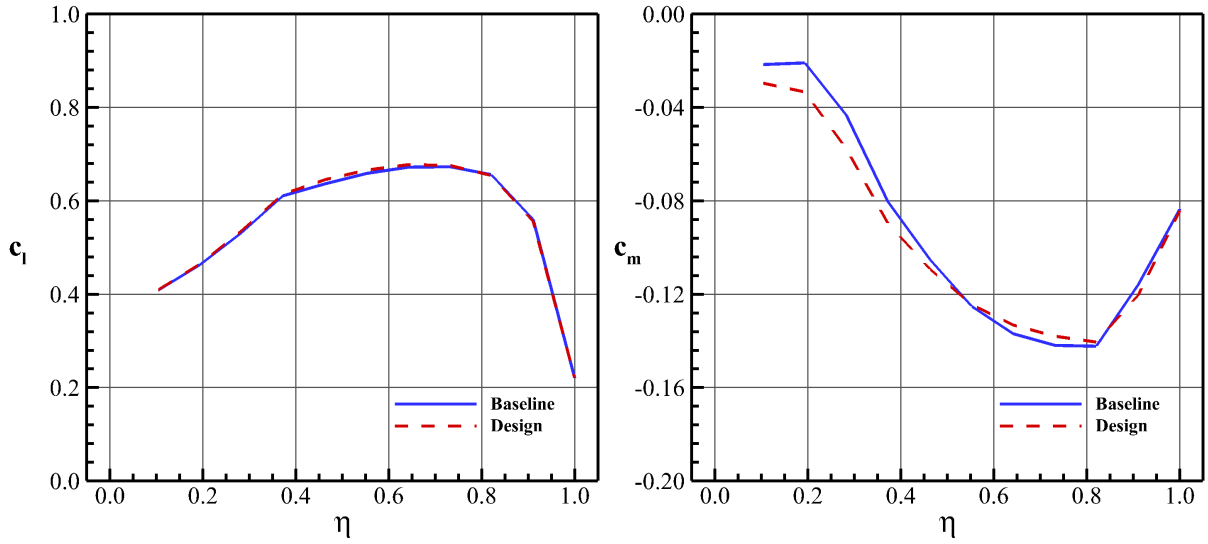

(a) Sectional lift coefficient

(b) Sectional pitching moment coefficient

Figure 7. USM3D results for the spanwise loading characteristics of the baseline and design CRMRS.

Figure 8 illustrates the spanwise variation in maximum thickness-to-chord ratio, $(t/c)_{max}$, twist , ϕ, and leading-edge radius normalized by local chord, $(r/c)_{LE}$. As expected, the maximum thickness-to-chord ratio is identical between the baseline and design as it was a user-specified constraint for structural considerations. However, the previous airfoil geometry illustrations show that the location of this maximum thickness is free to change its chordwise location. The twist was free to undergo slight changes to meet the target pressure distributions. Relative to the baseline, the twist is observed to slightly reduce inboard, increase midspan, and decrease again outboard toward the tip. The leading-edge radius proved to be the spanwise geometry characteristics with the most variability between the baseline and design. A reduction in leading-edge radius is observed across every wing design station, consistent with the previously noted decrease in leading-edge acceleration relative to the baseline.

Table 2 presents the final aerodynamic performance for the baseline and design CRMRS in terms of lift coefficient, drag coefficient, and the aerodynamic cruise efficiency parameter. The results show that CDISC is successful in reducing the baseline drag coefficient by 5 counts for a total savings of 2% with a corresponding cruise efficiency increment of ΔML/D = 0.36. It is important to note that these results assume a fully turbulent flow. By paper completion, the previously noted transition prediction software will be used to evaluate whether USM3D's forced-laminarization option should be used to any significant transition fronts to better model the resulting aerodynamic performance. Additionally, the APE drag evaluation software will be used to estimate the changes to the consitutent sources of total aircraft drag. An assessment of off-design performance will be included in the following slotted-wing section.

Table 2. Aerodynamic performance for the baseline and design CRMRS at cruise (M=0.8, Re_{MAC}=20x10^6).

Configuration	C_L	C_D	ML/D
Baseline	0.564	0.0257	17.54
Design	0.564	0.0252	17.90

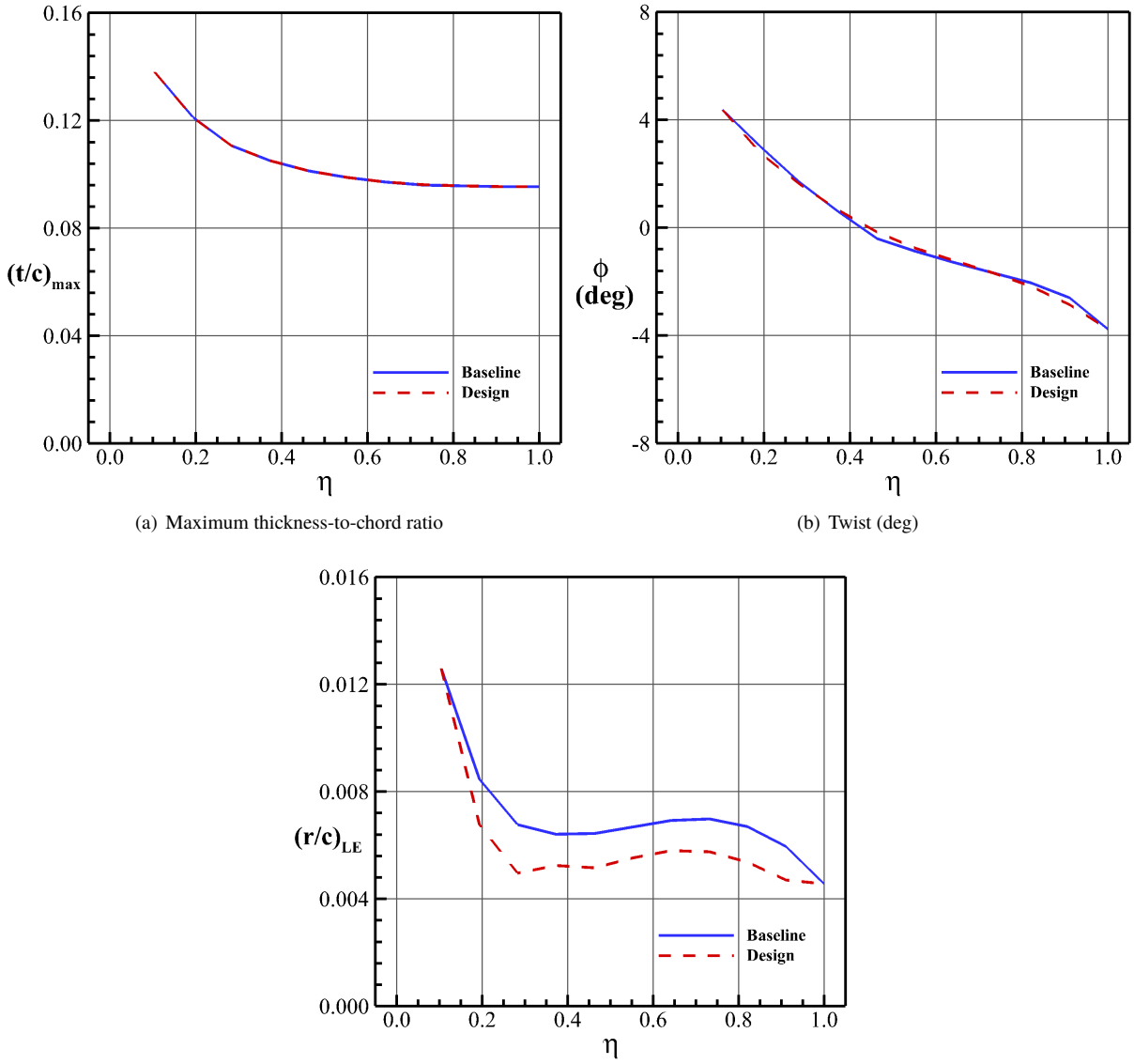

(a) Maximum thickness-to-chord ratio

(b) Twist (deg)

(c) Leading-edge radius normalized by local chord

Figure 8. USM3D results for the spanwise geometry characteristics of the baseline and design CRMRS.

IV. Slotted Wing Design

This section reviews the design and analysis of a slotted-wing variant of the reduced-sweep CRM, referred to as CRMRS-SW. The first subsection will review the slotted wing characteristics and baseline airfoil geometry. The following subsections will outline the strategy implemented within CDISC to explore the design, as well as cruise and off-design performance relative to the baseline CRMRS-SW and design CRMRS. Given the expected reduction in main airfoil element loading and the inherently lower Mach number and Reynolds number of the configuration, transition fronts will be predicted outside the design loop to better evaluate the slotted-wing's enabling potential for natural laminar flow.

A. Baseline Model and Design Condition

The CRMRS-SW is a partial-span, slotted-wing variant of the previously defined CRMRS aircraft configuration. A partial-span, slotted wing section extends from the planform break to the wingtip, comprising 63% of the semispan length. A conventional wing section, identical to the CRMRS, was used prior to the wing planform break. Additionally, a 3.5 inch gap was added between the conventional and slotted wing sections to eliminate a discrete transition in the airfoil geometry and improved computational grid quality. While a partial-span, slotted-wing design is considered in the present study, there are numerous embodiments of the cruise slotted wing technology that are worth exploring for future design studies, including: full-span slots, multiple partial-span slots, interchanging unslotted and slotted wing sections, etc. One benefit in investigating a partial-span design is that multidisciplinary risks may be reduced, as the technology would not interfere with the low-speed control surfaces, landing gear, or fuel tanks that are typically integrated into the inboard section of the wing.

Figure 9 illustrates a planform view of the CRMRS-SW with a series of 13 wing stations as indicated by red and black lines. Design stations 1-3 are consistent between the conventional and slotted wing configurations. Design stations 4 and 5 were defined just inboard and outboard, respectively, of the wing planform break. Design stations 6-13 span the total chord of the outboard slotted-wing section. CDISC will be used to shape the airfoils at each of these wing design stations to match target pressure distributions while satisfying a series of flow and geometry constraints in an attempt to reduce total aircraft drag at the design cruise condition. Since the aerodynamic performance of the CRMRS-SW is to be compared to the conventional CRMRS, it will be designed to the same cruise conditions, which have been tentatively set as a Mach number of 0.8, a Reynolds number based on MAC of 20 million, and a lift coefficient of 0.564.

The baseline slotted airfoil is characterized by two airfoil components: a main (fore) wing element and a flap (aft) wing element. Figure 10 illustrates the baseline slotted airfoil section at design station 9. Here, the main element extends from the leading edge to approximately 0.8c, and the flap element extends from 0.75c to the trailing edge, resulting in a 0.05c overhang between the two airfoil components. The twist for the main and flap components at station 9 are approximately -5° and -0.3°, respectively. The length, twist, and curvature of these two airfoil components implicitly define the resulting slot, which extends from about 0.7c to 0.8c.

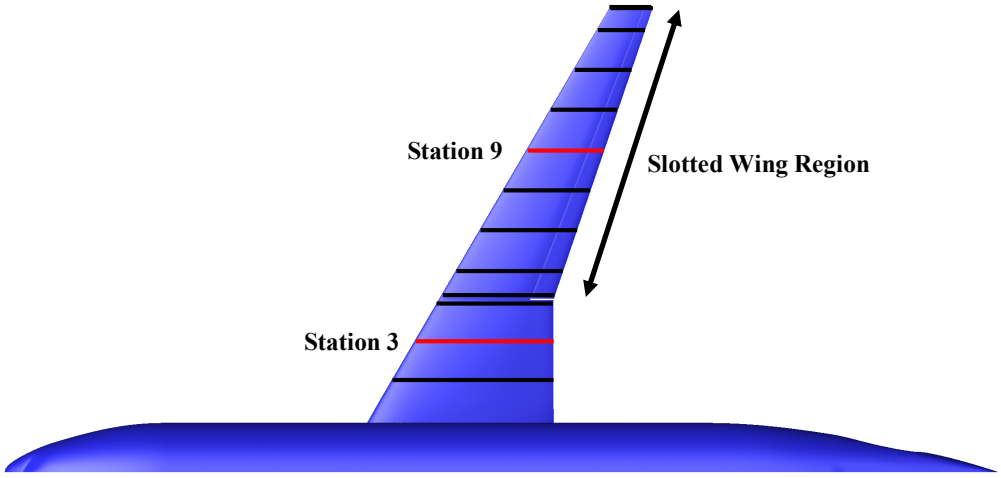

Figure 9. Planform view of the CRMRS-SW with wing design stations designated by black and red lines.

B. Design Strategy

The present research aims to evaluate the cruise slotted wing's potential for improving the aerodynamic efficiency of a generic transonic single-aisle aircraft through reductions in total aircraft drag. In support of this objective, a design strategy has been formulated to answer the three following questions:

1) Can a target pressure distribution be defined for a slotted airfoil that will yield a net reduction in total aircraft drag relative to a conventional transonic design?
2) Can a geometry be designed to match the target pressure distributions with sufficient accuracy while matching geometry constraints (thickness, leading-edge radius, twist, etc.)?
3) What are the off-design aerodynamic performance characteristics of the cruise slotted wing design?

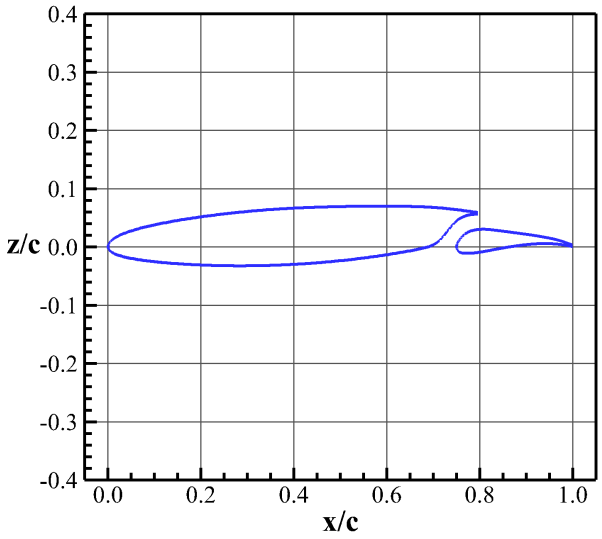

Figure 10. Baseline slotted wing airfoil at design station 9 for CRMRS-SW configuration.

The remainder of this section outlines the design strategy used to answer the proposed questions. The scope of this study is confined to evaluating the aerodynamic merit of the slotted-wing concept as applied to a single-aisle transonic transport configuration. If the concept shows increased promise, future studies would be needed to address any multidisciplinary risks prior to production applications. Additionally, a formal grid sensitivity study would be needed to reduce computational design uncertainty.

To enable a more extensive design exploration of the cruise slotted wing concept, USM3D will first be run using a quasi-2D (Q2D) conical flow (2.5D) approach [25]. The "2.5D" approach generates CFD solutions for a constant airfoil section scaled in the spanwise direction by a single sweep value for both the leading and trailing edges, i.e., an infinite swept wing. A Q2D grid generation method [26] was used to create a 0.02c wide grid using the airfoil section at design station 9 with the leading and trailing edge points on the parallel boundary plane sheared to match the 25° sweep at 0.6c. Design station 9 is located at a spanwise location midway along the slotted-wing region and was chosen to avoid any potential planform-break or tip effects that are not representative of the bulk slotted-wing behavior. For the Q2D USM3D solutions, periodic boundary conditions are to be used on the vertical planes in place of typical symmetry plane conditions. This approach has been used in previous design studies [23, 25] and represents a good approximation to 3D flow solutions when the wing flow isobars approximate lines of constant x/c. Such a flow feature is common to well-designed turbulent wings with single-shock structures.

For the initial design exploration, the transonic flow constraint used by CDISC to design the conventional wing will be applied separately to both the main and flap components of the slotted airfoil. Figure 11 illustrates the parameterization of this flow constraint to generate a target pressure distribution for the CRMRS-SW turbulent wing station design. This notional pressure distribution [8, 9, 27] reflects the theoretical basis for the slotted airfoil and will serve as a starting point for performance evaluations with the expectation that the design exploration study may lead to additional insights as to what constitutes an appropriate slotted-airfoil target pressure distribution. To reiterate its function, the slotted airfoil includes a slot between the lower surface of the main-element trailing edge and the upper surface of the flap-element leading edge to introduce stream air to the low-momentum, upper-surface boundary layer with the goal of reducing shock-induced separation on both surfaces. In addition, the camber of these two airfoil components are to be shaped in an attempt to reduce shock strength on each component. By introducing this high-momentum stream air to the upper surface boundary layer, a stronger pressure recovery on the flap element may be achieved, permitting greater loading.

The mechanisms by which the slot prevents boundary-layer separation have been detailed in prior studies [8, 9, 27] and are described here in relation to the CDISC flow constraint parameters illustrated in Fig. 11. The pressure distributions and variables associated with the main (M) and flap (F) airfoil components are denoted in blue and red, respectively. A dashed line is included to denote the critical pressure coefficient. As done for conventional wings, the flow on the upper surface of the main element is rapidly accelerated to a point X^{M}_{acc}, after which an adverse pressure gradient (V^{M}_{1}) is prescribed to produce a weak shock at a location X^{M}_{shk} that roughly coincides with the entrance of the

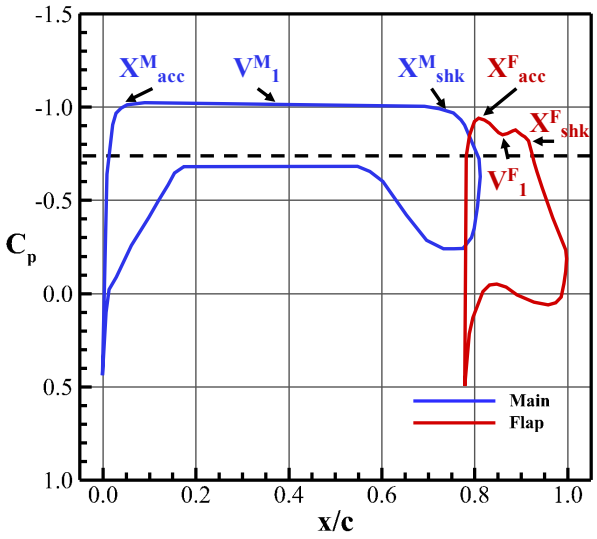

Figure 11. Notional target pressure distribution for CRMRS-SW turbulent wing station design.

slot. Due to the main element's highly cambered lower surface, the flow accelerates to near sonic levels, resulting in a pressure coefficient that is strongly negative relative to traditional supercritical airfoils. At the main-element trailing edge, the upper- and lower-surface boundary layers would ideally combine to form a wake that traverses above the flap element's upper surface, distinct from the flap boundary layer. In effect, the wake primarily recovers the aft-chord pressure gradient and remains resistant to flow reversal due to turbulent mixing. Simultaneously, the flow on the upper surface of the flap element is rapidly accelerated to a point X^F_{acc} that coincides with the slot exit and is then decelerated (V^F_1) to reduce the strength of a shock located at X^F_{shk}. The upper-surface boundary layer on the flap remains fairly thin when it encounters the shock due to its relatively short chord length. Pairing this benefit with the wake generated from the main element results in an ability to provide a steeper pressure recovery without boundary-layer separation.

If the skin-friction drag associated with the slot can be mitigated, the slotted airfoil may permit a net decrease in total drag due to reductions in wave drag. Furthermore, the increased loading on the flap element would allow for lower velocities on the main element, which could lead to greater extents of natural laminar flow. The Q2D flow solutions will be used in conjunction with CDISC to explore the impact of typical airfoil shaping parameters, flap location and deflection, and the relative loading between the two airfoil components on the pressure distribution profiles. Once suitable CDISC flow and geometry constraints are determined using the Q2D approach, the CRMRS-SW will be designed to the target pressure distributions using standard USM3D solutions.

C. Design Results

The current section provides results at select design stations on the inboard unslotted and outboard slotted wing regions for the baseline and design CRMRS-SW. Since the design exploration has yet to be completed, only the baseline results are provided. An initial baseline analysis was conducted by first simulating 2,000 flow solver iterations with flux-limiting on to stabilize the high-gradient slot region, followed by 8,000 flow solver iterations without flux-limiting. The angle-of-attack value needed to match the cruise lift coefficient was 2.3°.

Figure 12 shows the pressure distribution and airfoil geometry at design station 3 for the baseline CRMRS-SW. Design station 3 is consistent between the CRMRS and CRMRS-SW configurations, and thus, share the same baseline characteristics. A strong leading-edge acceleration is observed that leads to a rapid increase in local Mach number on the upper surface resulting in a strong shock that terminates at 0.4c. The baseline airfoil geometry shows a maximum thickness consistent with the shock-onset location followed by a highly cambered trailing edge to recover an aft loading.

Figure 13 illustrates the pressure distribution and airfoil geometry at design station 9 for the baseline CRMRS-SW. Design station 9, as previously noted in Fig. 9, is at a spanwise location midway along the outboard slotted-wing region. Results for the main and flap airfoil components are designated in blue and red, respectively. For the airfoil shape, local twist has not been removed to preserve the relative orientation between the main and flap elements that implicitly define the slot. The baseline pressure distribution on the main element is characterized by a rapid flow acceleration on the

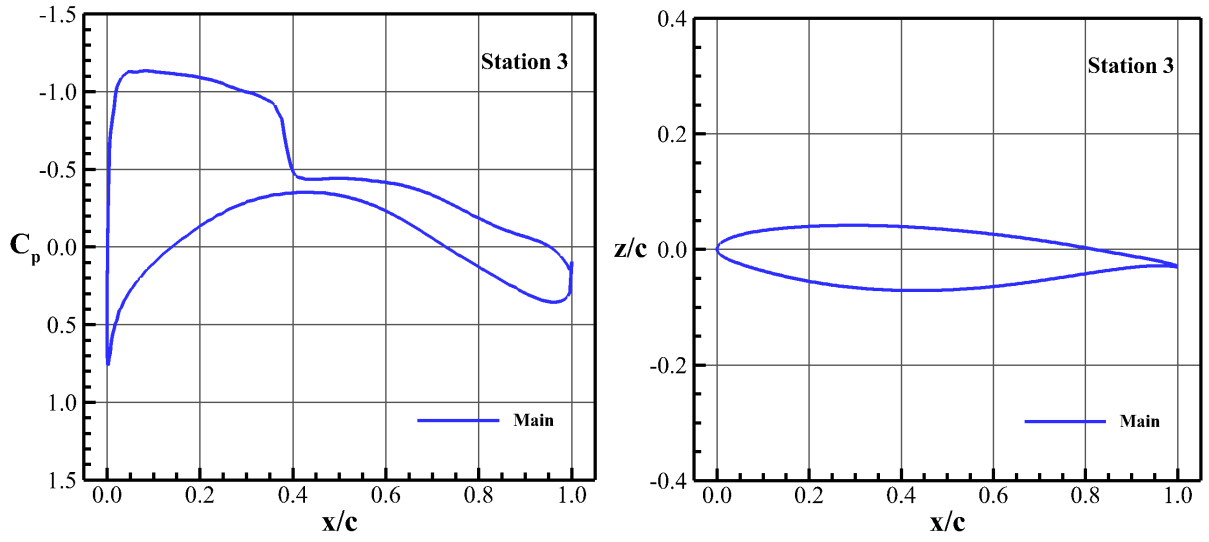

(a) Pressure distributions

(b) Airfoil geometries

Figure 12. USM3D results for the CRMRS-SW at Station 3 ($\eta = 0.28$). Left shows the baseline pressure distribution. Right shows the baseline airfoil geometry.

upper surface to a location of 0.05c followed by two shocks at chordwise locations of 0.35c and 0.65c. The flow on the lower surface of the main element encounters an acceleration to approximately midchord followed by a gradual reduction in velocity due to a mild, negative surface curvature. An abrupt change in curvature near the slot entrance on the lower surface of the main element leads to apparent flow separation at 0.7c, after which the flow reaccelerates to a near sonic trailing-edge "dumping" velocity. Improvements to the baseline main element can be made by introducing a more gradual curvature leading into the slot entrance to reduce flow separation and by tailoring the upper surface curvature to produce a single, weak shock without overcompression near the trailing edge. As for the flap element, the pressure characteristics on the lower surface are representative of those shown in the target pressure distribution of Fig. 11. The flow on the upper surface encounters a less than desirable acceleration through the slot that leads to a poor leading-edge loading. In addition to shaping the airfoil, the flap location and deflection angle will be parameterized to investigate their influence on the fore loading of the flap.

Additional comparisons of the spanwise loading and geometry characteristics between the baseline and design CRMRS-SW configurations are to be made in the final paper, whereas the current paper only includes baseline results. Figure 14 illustrates the spanwise variation in c_l and c_m, where the blue and red lines denote the main and flap airfoil component characteristics. Given that the CRMRS-SW is a partial-span, slotted wing configuration, the flap results are only relevant for $\eta > 0.38$. The spanwise behavior of c_l is qualitatively similar between the main and flap elements. The total c_l contribution between the main and flap components is approximately 80% and 20%, respectively, using a chord-based scaling. The spanwise variation in c_m on the main element shows an abrupt increase due to the immediate reduction in chord when transitioning from the unslotted to slotted wing regions. The pitching moment then shows a gradual decrease in pitching moment as a double-shock feature manifests on the upper surface, followed by a large increase due to tip effects. For the flap element, the shock on the upper surface tends to shift aft for successive outboard stations leading to a decrease in c_m. The value of c_m increases near the tip as loading is reduced.

Figure 15 shows the spanwise variation in maximum thickness-to-chord ratio, twist, and leading-edge radius for the baseline CRMRS-SW. The maximum thickness-to-chord ratio on the main element is drastically increased in the transition to the slotted-wing region as a result of the decrease in chord length. The thickness values for the flap component are larger due to the its smaller chord length. The twist on the main element depicts a generally linear decrease from the root to the tip with a negative jump in the transition from the unslotted- to slotted-wing region. On the flap element, the twist remains relatively low until reaching the design stations near the tip. This outboard reduction in twist supports the rapid increase in pitching moment near the wingtip. Finally, the leading-edge radius results show an expected discrepancy between the main and flap elements due to normalization by each component's local chord.

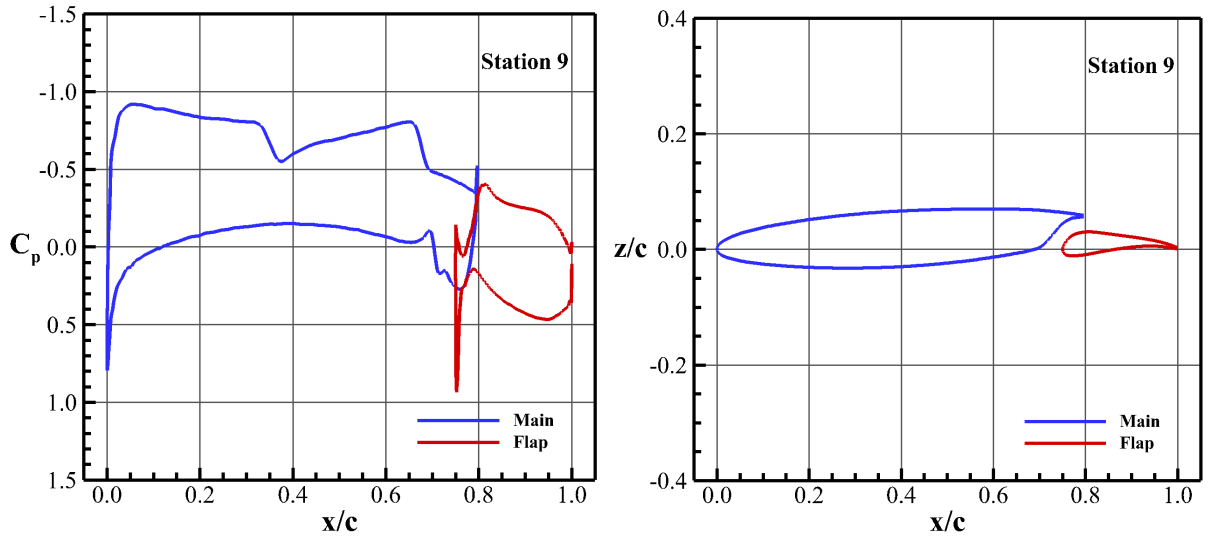

(a) Pressure distributions (b) Airfoil geometries

Figure 13. USM3D results for the CRMRS-SW at Station 9 ($\eta = 0.69$). Left shows the baseline pressure distribution. Right shows the baseline airfoil geometry.

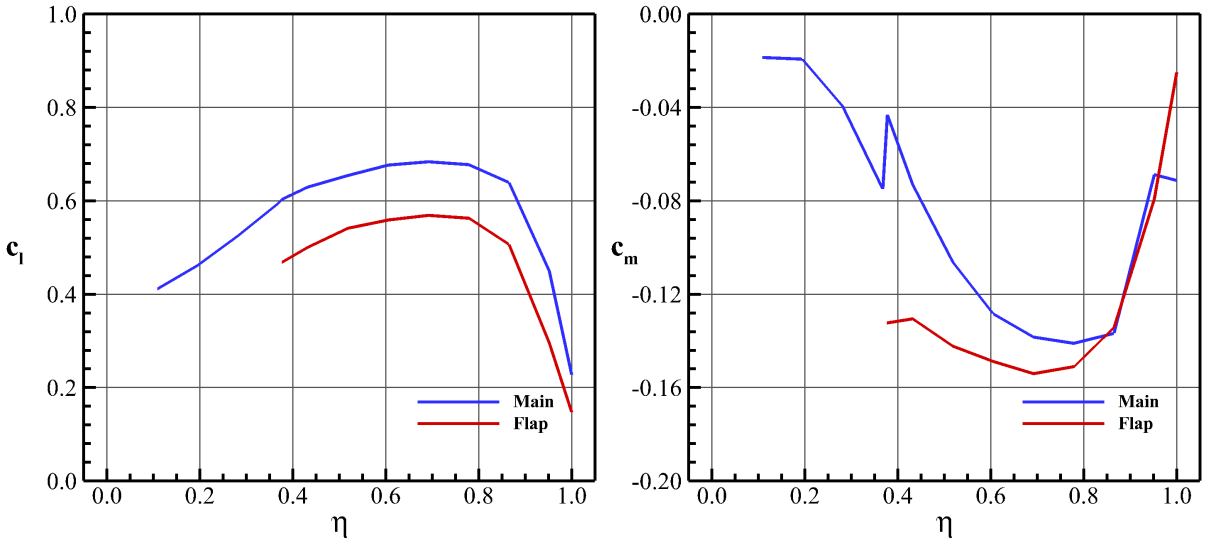

(a) Sectional lift coefficient (b) Sectional pitching moment coefficient

Figure 14. USM3D results for the spanwise loading characteristics of the baseline CRMRS-SW.

D. Off-Design Analyses

A series of off-design analyses are to be included in the final paper to better characterize the aerodynamic performance between the baseline and design CRMRS-SW, and, more importantly, establish the potential benefits of the slotted-wing relative to a conventional transonic wing. Results are to be presented in the form of drag polars for near-cruise and low-speed, high-lift flight conditions and a drag-divergence analysis at the design lift coefficient. Additionally, hinge moments due to flap loading will be provided in consideration of bracket sizing and weight concerns. If transition predictions suggest that the cruise slotted wing concept enables significant extents of natural laminar flow on the main airfoil element, the forced-relaminarization option in USM3D will be used for the subsequent analyses.

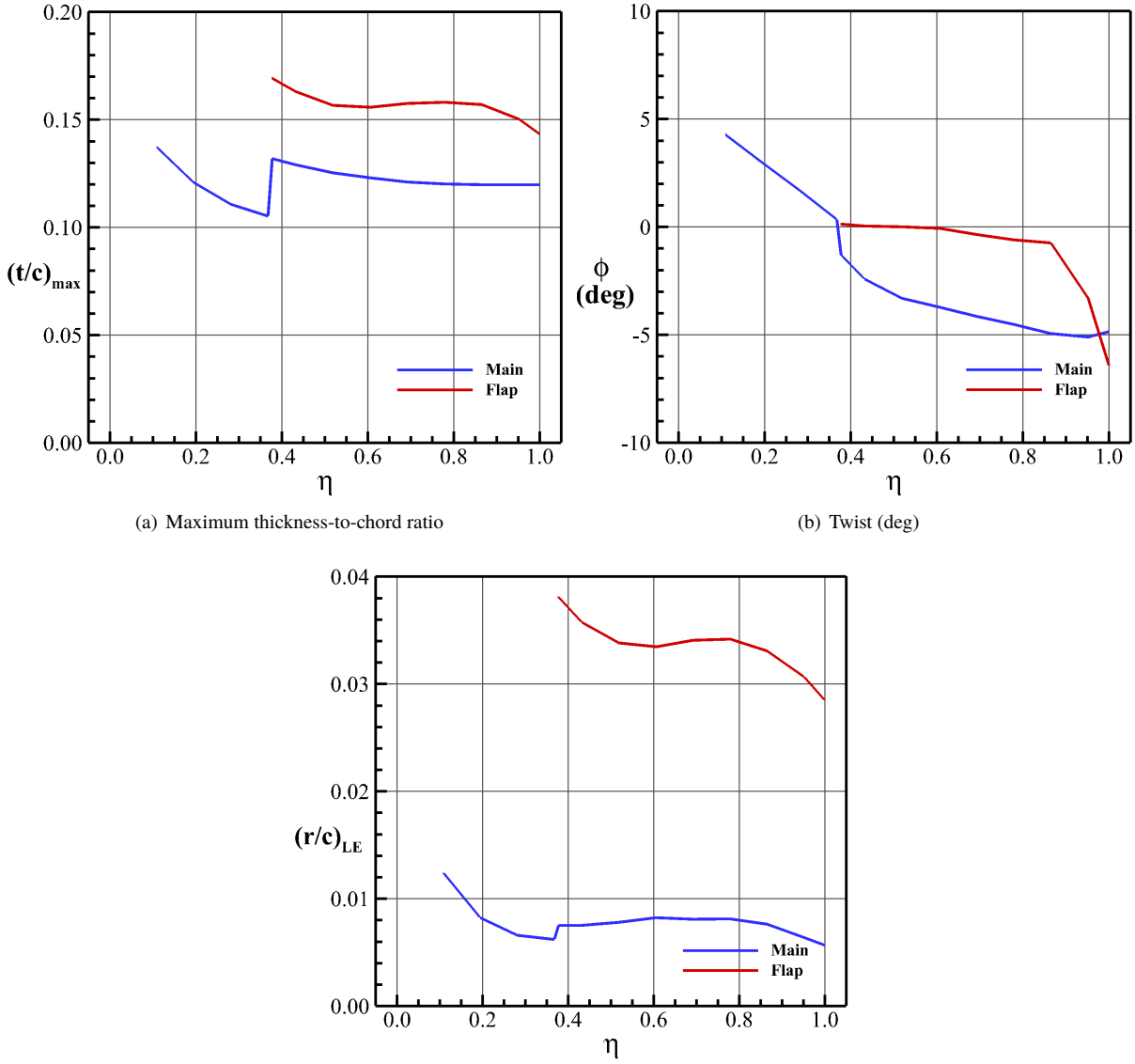

(a) Maximum thickness-to-chord ratio

(b) Twist (deg)

(c) Leading-edge radius normalized by local chord

Figure 15. USM3D results for the spanwise geometry characteristics of the baseline CRMRS-SW.

1. Near-Cruise Analysis

To investigate off-design cruise peformance, a series of fully turbulent USM3D solutions are to be generated by changing the configuration angle of attack to achieve a ±10% change in C_L about the baseline value of 0.564. The Reynolds number and Mach number will be held constant. A cruise drag polar will be provided to quantify the variability in aerodynamic efficiency as a function of angle of attack. Additionally, baseline and design pressure distributions will be provided for design stations 3 and 8 at the minimum, design, and maximum angles of attack to understand the flowfield impact on shock location and strength.

2. Low-Speed, High-Lift Analysis

To investigate the low-speed, high-lift conditions associated with takeoff performance, a series of fully turbulent USM3D solutions are to be generated for an angle-of-attack range of [10° to 30°] at a low-speed Mach number of 0.2 and a Reynolds number consistent with sea-level conditions. No high-lift leading or trailing edge devices are to be

added to the CRMRS configuration. The goal of this analysis is to identify any unsatisfactory high-lift characteristics, such as abrupt stall, that would warrant inclusion of leading-edge devices for improved performance.

3. Drag-Divergence Analysis

To evaluate any changes in the drag-divergence Mach number, a series of fully turbulent USM3D solutions are to be generated for a Mach number range of [0.6 to 0.9] while changing the configuration angle of attack accordingly to match the cruise lift coefficient value of 0.564. The results for the Mach number sweep will quantify the variability in total aircraft drag and potentially identify increases in wave drag at off-design conditions. Pressure distributions may be provided at design stations 3 and 9 for the range of simulated Mach numbers to better understand changes in shock movement or strength.

V. Conclusions

Given the desire to reduce the environmental impact of commercial transport aircraft, the aerospace industry is in continuous pursuit of configurations and technologies aimed at significantly reducing the noise, emissions, and fuel consumption of next-generation vehicles. In particular, fuel consumption reductions may be achieved by reducing an aircraft's empty weight and/or increasing its aerodynamic cruise efficiency. One potential concept targetting efficiency improvements is the cruise slotted wing. Slotted airfoils include a slot between the upper and lower surfaces near the trailing edge of a forward main airfoil component to introduce stream air to the low-momentum, upper-surface boundary layer on an aft flap airfoil component with the goal of reducing shock-induced separation on both surfaces. Also, the camber of the main and flap airfoil components can be designed to reduce shock-wave energy losses associated with the vertical extent of the supersonic region above the upper surface. These flowfield benefits may be realized at the vehicle level through a tradespace that includes the following design options: increasing cruise Mach number, increasing wing thickness, decreasing wing sweep, increasing lift coefficient and/or decreasing drag coefficient. The overarching goal of this research is to improve confidence in the application of the cruise slotted wing concept to single-aisle commercial transport configurations by focusing the technology's potential for total aircraft drag reduction at a given cruise condition.

Toward this effort, a new generic baseline configuration was created by reducing the sweep of the Common Research Model for a corresponding cruise Mach number of $M = 0.8$. The present study seeks to explore and compare the aerodynamic design of conventional and slotted-wing variants of the CRMRS using CDISC, a knowledge-based aerodynamic design method. To enable a more extensive design exploration of the cruise slotted wing concept, USM3D will first be run using a quasi-2D conical flow (2.5D) approach that approximates the 3D soluting using an infinite swep wing assumption. The quasi-2D flow solutions will be used in conjunction with CDISC to explore the impact of typical airfoil shaping parameters, flap location and deflection, and the relative loading between the two airfoil components on the pressure distribution profiles. Once suitable CDISC flow and geometry constraints are determined using the Q2D approach, the CRMRS-SW will be designed to the target pressure distributions using standard USM3D solutions. Design results for the proposed cruise condition are to be compared relative to the baseline configurations using wing station pressure distributions and geometries, as well as a quantitative evaluation of the individual components of total aircraft drag. Off-design results are to be presented in the form of drag polars for near-cruise and low-speed, high-lift flight conditions and a drag-divergence analysis at the design lift coefficient. A successful design study would establish the motivation for future exploration of the slotted wing concept in the form of numerical optimization, multiobjective/multidisciplinary trade studies, and experimental investigations.

Acknowledgments

This research is being conducted as part of the High Apsect Ratio Wing (HARW) Subproject work within the NASA Advanced Air Transportation Technology (AATT) Project. The authors would like to acknowledge Dr. Steve Krist and Dr. Richard Wahls of the NASA Langley Research Center for their valuable insights and feedback during the formulation of this study.

References

[1] Bezos-O'Connor, G., Mangelsdorf, M., Nickol, C., Maliska, H., Washburn, A., and Wahls, R., "Fuel Efficiencies through Airframe Improvements," AIAA Paper 2011-3530, June 2011. https://doi.org/10.2514/6.2011-3530.

[2] Joslin, R. D., "Overview of Laminar Flow Control," NASA/TP-1998-208705, October 1998.

[3] Wahls, R., "High Speed Slotted Wing Technology," *NASA Vehicle Systems Program Annual Meeting*, 2004.

[4] Whitcomb, R. T., and Clark, L. R., "An Airfoil Shape for Efficient Flight at Supercritical Mach Numbers," NASA/TM-X-1109, July 1965.

[5] Whitcomb, R. T., "Review of NASA Supercritical Airfoils," 9th International Council of the Aeronautical Sciences Congress, August 1974.

[6] Harris, C. D., "NASA Supercritical Airfoils: A Matrix of Family-Related Airfoils," NASA/TP-1990-2969, March 1990.

[7] Drela, M., "Design and Optimization Method for Multi-Element Airfoils," AIAA Paper 1993-969, February 1993. https://doi.org/10.2514/6.1993-969.

[8] McLean, J. D., Witkowski, D. P., and Campbell, R. L., "Slotted Aircraft Wing," U.S. Patent No. 7,048,235, May 2006.

[9] Vassberg, J. C., Gea, L.-M., McLean, J. D., Witowski, D. P., Krist, S. E., and Campbell, R. L., "Slotted Aircraft Wing," U.S. Patent No. 7,048,228. May 2006.

[10] Somers, D. M., and Maughmer, M. D., "Design and Experimental Results for the S414 Airfoil," U.S. Army Research, Development, and Engineering Command/W911W6-07-C-0047, August 2010.

[11] Somers, D. M., "An Exploratory Investigation of a Slotted, Natural-Laminar-Flow Airfoil," NASA/CR-2012-217560, April 2012.

[12] Somers, D. M., "Design of a Slotted, Natural-Laminar-Flow Airfoil for Business-Jet Applications," NASA/CR-2012-217559, July 2012.

[13] Somers, D. M., "Design of a Slotted, Natural-Laminar-Flow Airfoil for a Transport Aircraft," NASA/CR-2019-220403, August 2019.

[14] Coder, J. G., Maughmer, M. D., and Somers, D. M., "Theoretical and Experimental Results for the S414, Slotted, Natural-Laminar-Flow Airfoil," *AIAA Journal of Aircraft*, Vol. 51, No. 6, 2014, pp. 1883–1890. https://doi.org/10.2514/1.C032566.

[15] Maughmer, M. D., Coder, J. G., and Somers, D. M., "Exploration of a Slotted, Natural-Laminar-Flow Airfoil Concept," AIAA Paper 2018-3815, June 2018. https://doi.org/10.2514/6.2018-3815.

[16] Ortiz-Melendez, H. D., Coder, J. G., and Shmilovich, A., "High-Lift Simulations of Slotted, Natural-Laminar-Flow Airfoils," AIAA Paper 2019-0290, January 2019. https://doi.org/10.2514/6.2019-0290.

[17] Vassberg, J. C., DeHaan, M. A., Rivers, M. S., and Wahls, R. A., "Retrospective on the Common Research Model for Computational Fluid Dynamics Validation Studies," *Journal of Aircraft*, Vol. 55, No. 4, 2018, pp. 1325–1337. https://doi.org/10.2514/1.C034906.

[18] Frink, N. T., Pirzadeh, S. Z., Parikh, P. C., Pandya, M. J., and Bhat, M., "The NASA Tetrahedral Unstructured Software System (TetrUSS)," *The Aeronautical Journal*, Vol. 104, No. 1040, 2000, pp. 491–499.

[19] Campbell, R., "Efficient Viscous Design of Realistic Aircraft Configurations," AIAA Paper 1998-2539, June 1998. https://doi.org/10.2514/6.1998-2539.

[20] Wie, Y.-S., "BLSTA: A Boundary Layer Code for Stability Analysis," NASA/CR-1992-4481, December 1992.

[21] Chang, C.-L., "The Langley Stability and Transition Analysis Codes (LASTRAC): LST, Linear & Nonlinear PSE for 2D, Axisymmetric, and Infinite Swept Wing Boundary Layers," AIAA Paper 2003-974, January 2003. https://doi.org/10.2514/6.2003-974.

[22] Campbell, R. L., and Lynde, M. N., "Natural Laminar Flow Design for Wings with Moderate Sweep," AIAA Paper 2016-4326, June 2016. https://doi.org/10.2514/6.2016-4326.

[23] Campbell, R. L., and Lynde, M. N., "A Knowledge-Based Optimization Method for Aerodynamic Design," AIAA Paper 2019-1207, January 2019. https://doi.org/10.2514/6.2019-1207.

[24] Lynde, M. N., and Campbell, R. L., "Computational Design and Analysis of a Transonic Natural Laminar Flow Wing for a Wind Tunnel Model," AIAA Paper 2017-3058, June 2017. https://doi.org/10.2514/6.2017-3058.

[25] Streit, T., Wichmann, G., von Knoblauch zu Hatzbach, F., and Campbell, R., "Implications of Conical Flow for Laminar Wing Design and Analysis," AIAA Paper 2011-3808, June 2011. https://doi.org/10.2514/6.2011-3808.

[26] Nayani, S., "Evaluation of Grid Modification Methods for On-and Off-Track Sonic Boom Analysis," AIAA Paper 2013-798, January 2013. https://doi.org/10.2514/6.2013-798.

[27] Kelley-Wickemeyer, R. H., Seidel, G. E., Anast, P. Z., and McLean, J. D., "Airplane with Unswept Slotted Cruise Wing Airfoil," U.S. Patent No. 6,293,497, September 2001.